

# MATHEMATICAL MODELLING OF MELTING OF THERMOPLASTICS IN A SINGLE SCREW PLASTICATING UNIT\*

L. HALÁSZ

National Defence Research Institute, Budapest

Received June 27, 1989

## Abstract

A new complex mathematical model has been developed for the melting zone of a single screw plasticating unit. It has been discussed the different melting mechanisms, the presented model is used to describe the different melting processes. The present analysis leads to significantly improved predictions of the length of melting zone, and the solid bed, pressure and temperature profile. It can give the location of the break up phenomenon. This conclusion is supported by experimental data.

From the solid polymer in the screw plasticating units a melt is formed in the melting zone of and transformed into a homogeneous mix in the homogenizing zone to suit the shaping processes that follow. From the point of view of the plasticating unit as an entity it is of utmost importance that the melting processes are restricted to a defined part of the screw assembly and that the undergoing processes remain stable. Investigation in terms of models of melting processes commenced during the middle 1960's however, under standing of complex processes and the formation of suitable mathematical models are the achievements of recent times.

In order to investigate the melting processes experimentally to the polymer a small quantity of dye was added, a steady state plasticating process was established with chosen parameters of operation, once a steady state process was established the screw abruptly stopped, while the barrel was cooled at very rapid rate. The end result was a fixed frozen state. After careful warming of the screw, the screw was removed from the barrel, while the frozen material was sliced into segments for further investigations. From the cut sections the length of the melting zone, and the solid bed width profile was established [1, 2].

Based on the experiment described above a model of melting processes were derived, this is depicted in Figure 1.

The first such model of the melting process was described by Tadmor and coworkers [3 and 4]. The mechanism of the melting was investigated and found that the melting process takes place at the interface of the barrel

\* Dedicated to Prof. J. Giber on the occasion of his 60th birthday.

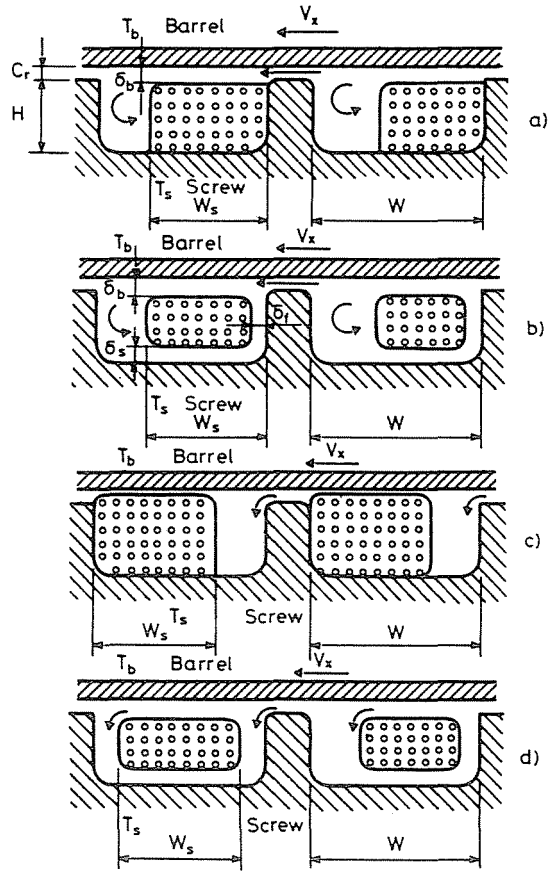


Fig. 1. Melting models

surfaces and the solid polymer. The solid polymer granulation in motion, moving from the feed hopper to the die, upon heating at the heated section of the barrel, the polymer is compacted into a solid plug. In the section, where the barrel surface temperature ( $T_b$ ) exceeds the melting point of the polymer ( $T_m$ ), melting takes place and a melt layer is formed on the surfaces of the barrel. The thickness of the melt on the surfaces of the barrel increases until it reaches a certain value and, upon continued melting of the polymer the melt pool is formed in the vicinity of the pushing flight of the screw. As the polymer proceeds in the channel the width of the melt pool is broadened and a circulating flow is developed around the solid bed. Reduced screw-depths resulted in modification of the above picture, since, due to the reduced screw depth a widening of the solid polymer is achieved. The melting process is considered complete at a point, where the width of the solid polymer became nought. In the model derived the melting processes were divided into two

distinct sections into the so called delayed section that lasted until the thickness of the molten film becomes constant at the barrel and into a melting section, where the width of the solid polymer is reduced and terminated at the point, where the solid polymer is eliminated, or entirely melted. The above model is depicted in part A of Figure 1 by way of illustration of the cross sections of two neighbouring channels.

The above described melting model was further developed [3 to 4], demonstrating that with an increase in the temperatures of the screw the melt formation is extended to the screw surfaces as well, thus, melting processes take place along the entire surface of the solid polymer. Examination of the melting processes were divided into relevant sections. The first section was the same as described by Tadmor, the delay section. The second phase constituted the section where melting took place on the surfaces of the barrel, in this case the melting processes were considered the same as was the case in the first section. In the third phase melting processes commenced on the screw surfaces as well and the thickness layer of the melt began to increase in size. In the fourth phase the growth of the melt layer ceases, a pressure flow is formed in the melt layer at the screw surfaces and circulation flow commences around the solid polymer.

Other authors described similar processes [5 through to 11]. These authors established that a melt film is formed on the surfaces of the barrel and on the surfaces of the screw following the delay section. The thickness of the melt film at the surfaces of the barrel changed in the direction of the axis of the screw channel and in a direction perpendicular to this axis. The thickness of the melt film at the screw surfaces changed only in the direction parallel with the axis of the screw channel. During the melting processes the width of the solid bed decreases, while the width of the melt pool increases. The melting processes are depicted in part B of Figure 1.

Klenk [12], later on Gale [13] and Chung [14] described a different type of melting mechanism, compared to above. Klenk and Gale, using rigid PVC powders observed and found a melting mechanism during processing, where melting processes took place in the section between the barrel and the screw flight of the screw in direction of its course, while the melt is accumulated in the vicinity of the trailing flight of the screw. In this particular case the melting process that took place was found to be slow, while the solid phase survived right to the tip of the screw. Klenk and Gale concluded that this type of occurrence of the melting processes was due to the fact that the rigid PVC material did not adhere to the wall surfaces. Gale also proved that the melting processes of PVC powders were substantially influenced by the quantities of additive materials added to improve flow characteristics of the polymer. Chung, with the aid of a model established, proved that the size of the clearance between the barrel and the flight of the screw also influenced

**Table 1**  
Different melting models

Models	Melting mechanisms		Solid polymer		Characteristics of the melting zone Rheological flow					Delay section	Break-up criteria
	Location of solid bed	Location of melt film	Mechanical Characteristics	Thermo Dynamic Characteristics	Melt film	Melt zone	Upper melt	Upper zone	Lower melt		
Halász (25)	<i>AM, K, PM</i>	<i>H, CS</i>	<i>CSD</i>	<i>RH, TH</i>	<i>H(T)</i>	<i>H(T)</i>	<i>2D, P</i>	<i>2D, P</i>	<i>2D, P</i>	+	+
Tadmor (3)	<i>AM</i>	<i>H</i>	<i>TM</i>	<i>RH</i>	<i>N</i>	—	<i>1D</i>	—	<i>1D</i>	—	—
Tadmor, Duvdevani, Klein (4)	<i>AM</i>	<i>H</i>	<i>TM</i>	<i>RH</i>	<i>H(T)</i>	—	<i>1D</i>	—	<i>1D</i>	+	—
Chung (14)	<i>AM</i>	<i>H</i>	<i>TM</i>	<i>RH</i>	<i>H(T)</i>	—	<i>1D</i>	—	<i>1D</i>	—	—
Donovan (19)	<i>AM</i>	<i>H</i>	<i>TM</i>	<i>RH, TH</i>	<i>H(T)</i>	—	<i>1D</i>	—	<i>1D</i>	—	—
Mondvai, Halász (5)	<i>AM</i>	<i>H, CS</i>	<i>TM</i>	<i>RH</i>	<i>H(T)</i>	—	<i>1D</i>	<i>1D</i>	<i>1D</i>	+	—
Halász (6)	<i>AM</i>	<i>H, CS</i>	<i>TM</i>	<i>RH, TH</i>	<i>H(T)</i>	—	<i>1D</i>	<i>1D</i>	<i>2D</i>	+	—
Edmonson, Fenner (8)	<i>AM</i>	<i>H, CS</i>	<i>FD</i>	<i>RH, TH</i>	<i>H(T)</i>	<i>N</i>	<i>1D</i>	<i>1D</i>	<i>2D, P</i>	—	—
Lindt (15)	<i>K</i>	<i>H, CS</i>	<i>TM</i>	<i>RH</i>	<i>H(T)</i>	—	<i>1D, P</i>	<i>1D, p</i>	—	—	—
Ba Sov, Kazankov (26)	<i>AM</i>	<i>H</i>	<i>TM</i>	<i>RH</i>	<i>H(T)</i>	<i>H(T)</i>	<i>1D, P</i>	—	<i>2D, P</i>	—	—
Shapiro, Halmos (9)	<i>AM</i>	<i>H, CS</i>	<i>FD</i>	<i>AH</i>	<i>H(T)</i>	<i>N</i>	<i>1D, P</i>	<i>1D, P</i>	<i>2D, P</i>	—	—
Fukase, Kunio (21)	<i>AM</i>	<i>H</i>	<i>TM</i>	<i>RH, TH</i>	<i>H(T)</i>	<i>H(T)</i>	<i>1D, P</i>	—	<i>1D, P</i>	—	—
Ebirli, Lindt (23)	<i>AM</i>	<i>H, CS</i>	<i>TM, FD</i>	<i>RH, TH</i>	<i>H(T)</i>	<i>H(T)</i>	<i>1D, P</i>	<i>1D, P</i>	<i>2D, P</i>	—	—
Lindt, Ebirli (24)	<i>AM</i>	<i>H, CS</i>	<i>TM, FD</i>	<i>RH, TH</i>	<i>H(T)</i>	<i>H(T)</i>	<i>1D, P</i>	<i>1D, P</i>	<i>2D, P</i>	—	—

*Legend:*

*AM* the solid bed at the active screw flight  
*PM* the solid bed at the passive screw flight  
*K* at the middle of the solid bed  
*H* melt layer at the surfaces of the barrel  
*CS* melt layer at the screw surfaces  
*TM* absolutely rigid  
*FD* freely deformable  
*CSM* reduced rigidity, with a tendency to break up  
*RH* radial heat conduction

*TH* heat transport in the direction of the axis  
*AH* with an average radial temperature  
*N* Newtonian  
*H(T)* power law as a function of temperature  
*1D* one dimensional flow  
*2D* two dimensional flow  
*P* pressure gradient  
 + taken into account  
 — not taken into account

the melting processes quite substantially. In case large clearances are employed, the melt tends to collect near the trailing screw flight. The melting processes observed by using rigid PVC material is shown by part C of Figure 1.

Lindt [15] using polypropylene and large extruder machinery described a melting process, where the melt formed a film around the solid polymer, while a completely filled melt pool did not form. The melt formed merely increased the film thickness of the polymer. In actual fact this phenomena seems to be the same melting process as was described earlier and labelled as phase two, here, melting takes place in a way that the melt commences circulation around the solid polymer. This case is depicted by part D of Figure 1.

The stability of the melting process ceases towards the termination of the melting processes and the solid bed begins to break up. This phenomena, in turn, causes pressure fluctuations in the processes. This process, instead of the type of mechanisms dealt with earlier, resembles a melting process, where each of the polymer particles floating in the melt are turned into fluid almost individually. The characteristic melting models are collected in Table 1.

In the above Table the melting mechanism is described together with the suppositions put forward with respect to the solid polymer, the rigid nature of the polymer and heating of the polymer, further, the suppositions and assumptions made with respect to the movement of the melt layers, finally, a description is provided dealing with the initial and the final phases of these melting zones.

The aim of this work is to form a complex model of melting processes, and to investigate the formation of break up. For this purpose, a comprehensive mathematical model has been developed contributing the process analysis based on the criteria parameters. The criteria parameters was summed in Table 2 [25].

The processes that take part in the melting zone, such as the formation of the actual melt layer on the surfaces of the barrel, followed by the formation of a melt layer on the screw surfaces, the development of one of the mechanisms of the melting processes, with other words at a point in time when the melting process extends to all boundary surfaces of the solid polymer, than, as the melting processes proceed, the quantity of the solid polymer left gradually decreases (indicated by the decrease of either the width, or the thickness, or both the thickness and the width of the solid bed), a situation might evolve, where the solid polymer begins to break up and solid polymer particles enter the melt of the screw channel, which float in the melt, finally, these floating polymer particles also melt and the entirety of the channel is filled with the melt. This means that in the metering zone the entirety of the screw channel is filled with melt and the homogenization of the melt is accomplished. In such a case the concurrent discussion of the processes of the two zones is fully justified, the movement of the melt present in either, or both zones are

**Table 2**  
Dimensionless Parameters Summary Table

Designation	Group	Definition
<i>Equation</i>		
Reynold's number	Momentum equation	$Re = \frac{\text{Inertia}}{\text{Internal friction}} = \frac{\rho Vx}{\mu}$
Euler number	Momentum equation	$Eu = \frac{\text{Pressure}}{\text{Inertia}} = \frac{\Delta P}{\rho V^2}$
Pressure parameter	Momentum equation	$Pr = \frac{\text{Pressure}}{\text{Internal friction}} = \frac{\Delta Px}{\Delta z \tau}$
Froude number	Momentum equation	$Fr = \frac{\text{Inertia}}{\text{Gravity}} = \frac{V^2}{xg}$
Peclet number	Energy equation	$Pe = \frac{\text{Heat transport}}{\text{Heat conduction}} = \frac{\rho CVx}{k}$
Greatz number	Energy equation	$Gz = \frac{\text{Heat transport}}{\text{Heat conduction}} = X Pc$
Brinkman number	Energy equation	$Br = \frac{\text{Dissipation}}{\text{Heat conduction}} = \frac{\overline{\tau \dot{\gamma}} x^2}{k(T_w - T_0)}$
Griffith number	Energy equation	$Gr = \frac{\text{Dissipation}}{\text{Heat conduction}} = \frac{b \overline{\tau \dot{\gamma}} x^2}{k}$
Deborah number	<i>Rheological state equation</i>	$N_{De} = \frac{\lambda_1 V}{L_0}$
Weissenberg number	Rheological state equation	$N_{we} = \frac{\lambda_1 V}{L_0}$
Parametric linearity number	Rheological state equation	$N_{pl} = \frac{\lambda_2 V}{L_0}$
<i>Physical state equation</i>		
Expansion number		$Ex = \kappa T^*$
Compressibility number		$Ko = \beta P^*$

Note:  $X = \frac{x}{L}$

Table 2. (cont.)

Designation	Group	Definition
<i>Others</i>		
Stefan number	Heat absorbed by the molten material Heat absorbed by the solid material	$St = \frac{\rho_m C_m AT}{\rho_s [A + C_s (T_m m - T_0)]}$
Bikerman number		$Bk = \frac{\text{adhesive force}}{\text{frictional force}} = \frac{\delta A}{fP}$
Bebris number		$Be = \frac{\text{external friction}}{\text{internal friction}} = \frac{f_{ou}}{f_{in}}$
Nusselt number (Biot number)		$Nu = \frac{\text{heat transfer}}{\text{heat conduction}} = \frac{ax}{k}$
Fouriernumber		$Fo = \frac{\text{heat conduction}}{\text{localized heat flow}} = \frac{at}{x^2}$

similar and only the geometry of the space the melt occupies differ from each other. The phases of the melt processes are:

- the development of the melt layer at the surfaces of the barrel,
- the main melting process,
- the breaking-up process, followed by a melting process.

Each of the part processes are:

- the formation of the melt layer at the surfaces of the barrel and the melt flow in the melt layer of the barrel surfaces,
- the movement of the solid bed till the appearance of the melt layer on the screw surfaces,
- the complete development of the melt layer at the screw surfaces, together with the appearance of melt flow in the screw surface layer, followed by circulation flow around the solid polymer,
- the movement of the solid bed surrounded by the melt,
- the melt flow in the clearance between the barrel and the screw flight (leakage flow),
- the melt flow along the solid polymer,
- the completion of melting of all floating solid particles,
- the melt flow filling the screw channel.

At the commencement of the melting processes the melt formed on the surfaces of the barrel first fills the porous gaps present in the solid polymer, followed

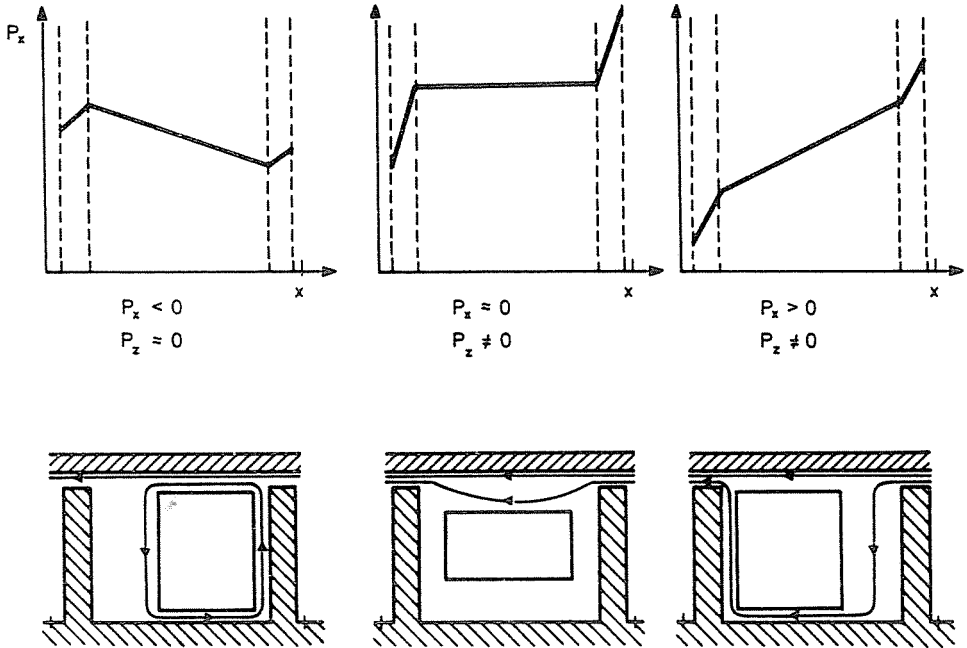


Fig. 2. Cross-channel pressure gradients of the various melting processes

by the formation of the melt layer, finally, melting takes place at the screw surfaces beyond the surfaces of the barrel in the first few turns of the screw. The very type of the melting process occurring depends upon the magnitude of the pressure gradient as the fact is illustrated by Figure 2. In case the pressure gradient in the channel, in a crosswise direction is negative, the width of the solid bed decreases and the melt formed is collected near the pushing screw flight. In case the pressure gradient is positive, the melting process that takes place is essentially the same as described above, but, the melt collects near the trailing screw flight, primarily, between the screw flight and the barrel, obtained from the melt flow across from the previous turn of the screw. In case the pressure gradient is near a zero value, melting takes place by increased thickness of the melt layer, primarily, at the surfaces of the barrel and at the surfaces of the screw. Out of the three possible mechanisms the choice lies in the crosswise pressure gradient.

The location of break-up constitutes of utmost importance.

The structure of the polymer resembles the form of a compressed granulation, the surfaces of the granulation are peppered with molten polymer particles, during the movement of the solid polymer on its surfaces bending moments and forces are acting. In case the differences in the bending moments applied exceed the solid cohesive forces of the polymer, the polymer breaks

up resulting in floating polymer particles in the melt. The break-up process of the polymer continues as long as the bending moments exceed the mechanical strength of the polymer. The criterion parameter of break-up is represented by the dimensionless number of the ratio  $Ba_1/Ba_2$ . In such a case the external force is the difference between the torque values at the barrel surfaces and at the screw surfaces. It is difficult to understand the cohesive strength of the solid polymer. The particles of the solid polymer present in the screw channel is compressed by the pressure gradient acting in the direction of the axis, due to the melting process the surface particles are sintered. The cohesive strength of the solid bed is best described by pressures in the direction of the axis.

**Table 3**

Dimensionless criteria parameters for the melting zone and for the metering zone

Process	Criteria parameter value ranges	Remarks
Melt layer at the surfaces of the barrel	$Re = \sim 10^{-5}$ $\sigma_p = 10^{-1} \dots 10^{-2}$ $G_z(x) = 10^{-3} \dots 10^{-2}$ $G_z(z) = 10^{-2} \dots 10^0$ $Br = 10^{-1} \dots 10^1$ $N_{De} = 10^{-2} \dots 10^{-1}$ $N_{We} = 10^{-1} \dots 10^0$ $N_{p1} = 10^1 \dots 10^3$	
Melt layer at the surfaces of the screw	$Re = 10^{-4}$ $\sigma_p = 10^{-1} \dots 10^0$ $G_z(x) = \sim 10^{-2}$ $G_z(z) = 10^{-3} \dots 10^{-1}$ $Br = 10^{-2} \dots 10^0$ $N_{De} = 10^{-3} \dots 10^{-2}$ $N_{We} = 10^{-2} \dots 10^{-1}$ $N_{p1} = 10^1 \dots 10^2$	
Melting zone	$Re = \sim 10^{-2}$ $\sigma_p = \sim 10^0$ $G_z(x) = 10^{-2} \dots 10^1$ $G_z(z) = 10^{-1} \dots 10^2$ $Br = 10^0 \dots 10^2$ $Na = 10^0 \dots 10^2$ $N_{De} = \sim 10^{-2}$ $N_{We} = 10^{-1} \dots 10^0$ $N_{p1} = 10^1 \dots 10^2$	

Table 3. (cont.)

Process	Criteria parameter value ranges	Remarks
Clearance at the barrel surfaces	$Re = 10^{-5}$	
	$\sigma_p = 10^2$	
	$G_z(x) = 10^{-2}$	
	$G_z(z) = \sim 10^0$	
	$Br = 10^0 \dots 10$	
	$N_{De} = 10^{-2} \dots 10^{-1}$	
	$N_{We} = 10^{-1} \dots 10^0$	
Metering zone	$N_{p1} = 10^1 \dots 10^3$	
	$Re = \sim 10^{-3}$	
	$\sigma_p = \sim 10^0$	
	$G_z(x) = 10^{-2} \dots 10^1$	
	$G_z(z) = 10^{-1} \dots 10^2$	
	$Br = 10^{-1} \dots 10^2$	
	$Na = 10^0 \dots 10$	
$N_{De} = \sim 10^{-2}$		
$N_{We} = 10^{-1} \dots 10^0$		
$N_{p1} = 10^1 \dots 10^2$		

The various zones of the melting process with their characteristic criteria are summarized in Table 3. The geometrical features are also listed in the same table. All aspects mentioned above with respect to the movement of the solid material does apply, provided that one considers that the process is one, where the entire surface area of the polymer is surrounded by a layer of melt, thus, the sliding friction is replaced by shearing stresses. The melting process influences the movement of the solid material in an indirect way, since the melting process is the determinant factor in the formation of the thickness of the melt layer. The criteria parameters relevant to the solid polymer is collated in Table 4.

Generally speaking, the thickness of the melt layer is ( $10^0 \dots 10^2$ ) Cr, apart from the initial phase, it is characterized by an even thickness. The melt layer possesses velocity vectors in the  $x$  and in the  $z$  directions, the small Reynolds number is an indication that the inertia is negligible, however, the value of the parameter  $\sigma_p$  is an indication that the affect of the pressure flow is not negligible in many instances, hence, the momentum equation constitutes the pressure gradients in the  $x$  and in the  $z$  directions together with the shearing stresses.

Examination of the Graetz numbers show that the heat transport in the  $z$  direction must be taken into account, furthermore, based on the Brinkman number the dissipation cannot be ignored. The Deborah number, the

**Table 4**  
Dimensionless parameters for melt conveying

Parameters	Definitions
Pressure gradient	$\pi_p = \frac{\partial PH}{\partial z \bar{\tau}}$
Coordinate	$Y = y/H$
Velocity in $x$ direktion	$\pi_{v_x} = v_x/V_z$
Velocity in $z$ direction	$\pi_{v_z} = v_z/V_z$
Volume flow rate	$\pi_Q = \frac{Q}{HV_z W}$
Pressure gradient ratio	$a_1 = \frac{\partial P/\partial x}{\partial P/\partial z}$
Bikerman-number	$Br = \frac{b\mu_0 V_z^{1+n}}{k_m J H^{n+1}}$
Temperature	$\pi_T = b(T - T_s)$ $G_Y = (Y - Y_1)^2 + a_1^2(Y - Y_2)^2$
average shear rate	$\dot{\gamma} = \frac{V_z}{H}$
average shear stress	$\bar{\tau} = \mu_0 \left  \frac{\dot{\gamma}}{\dot{\gamma}_0} \right ^{n-1} \exp [b(T_b - T_0)]$

Weissenberg number and the parametric linearity number indicate that the polymer in the melt layer is a viscous, non-Newtonian fluid.

Study of the expansion number shows that its magnitude is of the order of  $10^{-3}$ , which means that the physical state equation need not to be taken into account.

Upon examination of the Bikerman-number it is concluded that the Bikerman-number, in general, is a large number, although in some equations the Bikerman-number is close to the value of unity, which means that for some of the materials the sliding of the polymer along the wall need to be considered.

In the investigation of the flow at the clearance, the fact must be accounted for that the flow takes place between one moving and one stationary surface of metal. The flow space is characterized by the ratio of  $C_r/e \sim 0.005$ . In description of the flow by the momentum equation, apart from the shearing stresses in the  $z$  direction, all other members may be neglected, the flow constitutes a drag flow. The role of the pressure gradient in the crosswise direction in the screw channel, due to the pressure distribution, is important

to be considered. The heat transport may be ignored compared with the magnitude of heat conduction and heat dissipation. The affects of sliding at the surfaces of the barrel may be substantial.

The melt layer at the screw surfaces are, generally, thicker than the melt layer at the surfaces of the barrel, its thickness increases gradually in the  $z$  direction. The flow velocities at the screw surfaces is smaller than the flow velocities at the surfaces of the barrel, henceforth, the role played by the pressure gradient is more important. For the melt layer at the screw surfaces may be described by the system of equations related to the surfaces of the barrel. The zone filled with the melt is, initially, resembles a deep channel section  $\left(\frac{H}{W} \sim 0.2\right)$ , the affect of the curvature is also substantial  $\left(\frac{H}{D} \sim 0.2\right)$ , while the width of the zone upon progression of the melting process changes from 0 to  $W$ , which means that the ratio  $\frac{H}{W_m}$  changes from infinity to  $10^{-1}$ — $10^{-2}$  values. This, in actual fact means that all three constituent parts of the velocity values must be taken into account in the zone filled by the melt. In the momentum equation the force of inertia may be ignored and, in case the screw depths do not increase in an excessively rapid manner, the constituents of the normal stresses may also be rendered negligible (i.e.  $N_w$  is small). Upon consideration of the energy equation one concludes that the Graetz number cannot be ignored in either the  $z$  direction, or in the  $x$  direction, which means that both constituents of heat transport must be taken into account. The large Bikerman-number indicates that the affect of dissipation is also substantial. The melt does not behave as a Newtonian viscous liquid, it is an incompressible continuum, thus, the heat expansion may also be ignored. In boundary conditions, generally, the Bikerman number is large, thus the affect of sliding may be ignored. Upon establishing the boundary conditions of the energy equation it is customary to assume that heat transfer at the screw does not take place. A feature of the metering zone is that the flow takes place in a shallow channel, with values of  $H/W \sim 0.05$  and  $H/D \sim 0.05$ , hence in this case the affect of the curvature may be ignored. The criteria parameters characterizes the flow is contained in Table 4. The melting model constitutes the following major parts:

- a model describing the development of the melt layer at the surface of the barrel,

- a model, describing the main processes that take place during melting, including the criteria equation as part of the choice of the model, together with the melting process model, the break-up criterion equation, finally, the relationship describing the length of that part of the melt where the break-up process takes place, and

— the melt conveying models describing the deep and the shallow channels.

Based on analysis of the criterion parameter with respect to the metering zone, the melt flow may be described as a flow that takes place in a shallow channel.

The formation of the melt layer at the surfaces of the barrel.

The melt layer of increasing thickness at the barrel surfaces may be characterized by the field: velocity vector,  $\mathbf{v} = ((v_z(y, z); 0, v_y(y, z))$ . The corresponding balance equations are:

$$\frac{\partial y_z}{\partial z} + \frac{\partial v_y}{\partial y} = 0 \tag{1}$$

$$\frac{\partial P}{\partial z} = \frac{\partial \tau_{yz}}{\partial y} \tag{2}$$

$$\rho C_p \left( v_z \frac{\partial T}{\partial z} + V_y \frac{\partial T}{\partial y} \right) = k \frac{\partial^2 T}{\partial y^2} + \tau_{yz} \frac{\partial V_y}{\partial y} \tag{3}$$

The boundary conditions for solution of the equation are:

$$\begin{aligned} v_z = V; \quad v_y = 0; \quad T = T_f \quad \text{if } y = 0 \\ v_z = 0; \quad T = T_m \quad \text{if } y = \delta \end{aligned} \tag{4}$$

The energy balance at the interface of the solid and the molten material is given by:

$$k_m \frac{\partial T}{\partial y} - k_s \frac{\partial T}{\partial y} = \rho_s \lambda^* \left( V_y - V \frac{d\delta}{dz} \right) \tag{5}$$

where:  $\lambda^* = \lambda + C_p(T_m - T_0)$  represents the apparent heat conversion.

The mass balance, assuming constant melt densities is given by:

$$\rho_m \frac{d}{dz} \int_0^\delta v_z dy = \rho_s \left( V_y - V \frac{d\delta}{dz} \right) \tag{6}$$

The power law may be used as the rheological state equation, thus:

$$\eta = \mu, e^{-b(T - T_0)} \left| \frac{\partial v_z}{\partial y} \right|^{n-1} \tag{7}$$

The physical state equation need not to be taken into account. Rewriting equations (1) through to (7) in dimensionless formats yield the following relationships:

$$\frac{\partial \pi_{v_z}}{\partial Z} - \frac{1}{\Delta} \frac{d\Delta}{dZ} Y \frac{\partial \pi_{v_z}}{\partial Y} - \frac{1}{\Delta} \frac{\partial \pi_{v_y}}{\partial Y} = 0 \tag{8}$$

$$\frac{\partial}{\partial Y} \left[ \rho^{-\beta\pi_T} \left| \frac{\partial \pi_{v_z}}{\partial Y} \right|^{n-1} \frac{\partial \pi_{v_z}}{\partial Y} \right] = \Delta^{n+1} \frac{\partial \pi_p}{\partial Z} \quad (9)$$

and

$$\begin{aligned} Sf \left( \pi_{v_z} \frac{\partial \pi_T}{\partial Z} - \frac{1}{\Delta} \frac{d\Delta}{dZ} \pi_{v_z} Y \frac{\partial \pi}{\partial Y} + \frac{1}{\Delta} \pi_{v_y} \frac{\partial \pi_T}{\partial Y} \right) = \\ = \frac{1}{\Delta^2} \frac{\partial^2 \pi_T}{\partial Y^2} + \frac{Gn}{\Delta^{n+1}} \left| \frac{\partial \pi_v}{\partial Y} \right|^{n+1} e^{-\beta\pi_T} \end{aligned} \quad (10)$$

with limiting conditions

$$\begin{aligned} \pi_{v_z}(Z, 0) = 0; \quad \pi_{v_y}(Z, 0) = 0; \quad \pi_{v_z}(Z, 1) = 1 \\ \rho_m \pi_{v_y}(Z, 1) = \rho_s \pi_{v_y} (\rho_s - \rho_m) \frac{d\Delta}{dZ}; \quad \pi_T(Z, 0) = 1 \\ Z > 0; \quad \pi_T(Z, 1) = 0 \end{aligned} \quad (11)$$

$$\frac{\partial \pi_T}{\partial Y}(Z, 1) = \Delta \left( \pi_{v_y} - \frac{d\Delta}{dZ} \right) \quad (12)$$

$$\Delta = \frac{\delta}{\delta_0}; \quad Z = \frac{z}{l}; \quad Y = \frac{y}{\delta}$$

$$\pi_T = \frac{T - T_m}{T_f - T_m}; \quad \pi_{v_z} = \frac{v_z}{V}; \quad \pi_{v_y} = \frac{v_y l}{V \delta_0} \quad (13)$$

$$l = \rho_s \lambda^* V \delta_0^2 / k_m (T_f - T_m)$$

$$\pi_p = \frac{P k_m (T_f - T)}{\mu_1 \rho_s \lambda^* V^{n+1} \delta_0^{1-n}} \quad (14)$$

$$Sf = \frac{\rho_m C_m (T_f - T_m)}{\rho_s \lambda^*} \quad (15)$$

$$Gn = \mu_1 V^{n+1} \delta_0^{1+n} / k_m (T_f - T_m) \quad (16)$$

The above equation may be solved numerically. In case  $n=1$  (with other words, the melt is of Newtonian behaviour) and  $Gn \ll 1$ , which means that heat conduction dominates, the solution for equation (8) is given by:

$$\delta = \left( \frac{2Sf A k_m Z}{V} + \delta_0^2 \right)^{\frac{1}{2}} \quad (17)$$

where: "A" is a constant with a value of around unity. Determination of the initial value,  $\delta_0$  presents problems in the above equation. In the initial phases of the melting processes, at the point where the temperature at the surfaces

of the barrel reaches the melting point of the polymer (i.e.  $Z=0$  and  $\delta_b=0$ ), the melt formed first fills the gaps present between the particles, which means that at  $z=z_1$  a melt layer  $\delta=\delta_0$  is formed. Starting now from this approach and consideration the melting processes are, now, the same as described above.

The values of  $Z_1$  and  $\delta_0$  according to Kacir and Tadmor [27] are:

$$z_1 = 1.3 \frac{R}{\sqrt{K_0}} \frac{\rho_s V_s}{\rho_m V} \frac{K_1(1-e^{-K_1})}{K_1 - (1-e^{-K_1})} \quad (18)$$

and

$$\delta = 0.923 \sqrt{K_0 R} \quad (19)$$

where:  $R$  represents the radii of the particles, while  $K_0$  is given by:

$$K_0 = \frac{\pi}{2} \frac{\rho_s k_m S f}{\rho_m^2 C_m V} \frac{K_1(1-e^{-K_1})}{K_1 - (1-e^{-K_1})} - \frac{\mu V}{2\rho_m \lambda^*} \frac{K_1}{1-e^{-K_1}} \quad (20)$$

$$K_1 = \frac{b(T_w - T_m)}{n} \quad (21)$$

Once melting processes commenced the thickness of the melt layer increases rapidly, it grows to a thickness equivalent with the flight clearance.

The thickness layer of the melt continues to grow at a rate subject to operating circumstances and subject to the properties of the material under investigation, to a thickness described by the relationship:

$$\delta_b \int_0^1 (1 - \pi_{v_z}) dY = Cr \quad (22)$$

followed by a decrease of the width of the polymer. The width changes upon the affect of melting is given by:

$$wW_s = \frac{d}{dz} (\rho_s V_s W_s H) \quad (23)$$

Same may be expressed in terms of the cross flow, thus:

$$wW_s = \frac{1}{2} V_x \delta \rho_m - \frac{1}{2} V_x Cr \rho_m \quad (24)$$

The melt thickness may be, now, determined from equations (17), (23) and (24).

### The developed melting processes

All surfaces of the solid polymer is coated with a layer of the melt. The development of this particular phase commences at a time when melting begins to take place at the screw surfaces.

Similar considerations apply to the melt pool. During the initial phases of the melting process the characteristic feature of the process is that flow of the melt takes place in the deep channel. Ignoring the corrections due to the specific geometry of the channel introduces only a small error, as was shown earlier on, thus the movement of the melt may be represented by a model, mutually suited [28], henceforth:

$$\pi_{Qz} = \pi_p |\pi_p|^{\frac{1}{n}-1} \exp \frac{b\Delta T}{n} \int_0^1 (1-Y)(Y-Y_1) \exp \frac{\pi_T}{n} |G_T|^{\frac{1-n}{2n}} dY \quad (25)$$

$$\pi_{Qx} = 0. \quad (26)$$

$$1 = \pi_p |\pi_p|^{\frac{1}{n}-1} \exp \frac{b\Delta T}{n} \int_0^1 (Y-Y_1) \exp \frac{\pi_T}{n} |G_Y|^{\frac{1-n}{2n}} dY, \quad (27)$$

$$\operatorname{tg} \Theta = \alpha_1 \pi_p |\pi_p|^{\frac{1}{n}-1} \exp \frac{b\Delta T}{n} \int_0^1 (Y-Y_2) \exp \frac{\pi_T}{n} |G_Y|^{\frac{1-n}{2n}} dY. \quad (28)$$

$$Gz \pi_{v_z} \frac{\partial \pi_T}{\partial Z} = \frac{d^2 \pi_T}{dY} - Br |\pi_p|^{\frac{1}{n}+1} \exp \frac{b\Delta T}{n} \exp \frac{\pi_T}{n} |G_Y|^{\frac{1+n}{2n}} \quad (29)$$

where: the dimensionless quantities are collated and given by Table 4.

The boundary conditions of the equations, in order to make clear distinctions and to avoid confusion are written in their original forms as follow:

— in the melt layer at the barrel surfaces:

$$\begin{aligned} y=0, \quad v_z &= V_s, \quad V_x=0, \quad T=T_m \\ y=\delta_b, \quad v_z &= V_z, \quad v_x=-V_x, \quad T=T_b \\ z=z_1, \quad T &= T_{\text{entry}} \end{aligned} \quad (30)$$

— in the melt layer at the screw surfaces:

$$\begin{aligned} y=0, \quad v_z &= 0, \quad v_x=0, \quad T=T_m \\ y=\delta_s, \quad v_z &= V_s, \quad v_x=0, \quad T=T_m \\ z=z_2, \quad T &= T_{\text{entry}} \end{aligned} \quad (31)$$

— in the zone filled with the melt:

$$\begin{aligned} x=0, \quad v_z &= 0, \quad T=T_m \\ x=W-W_s, \quad v_z &= V_s, \quad T=T_m \end{aligned}$$

$$\begin{aligned}
 y=0, & \quad v_x=0, & \quad V_z=0, & \quad T=T_s \\
 y=H, & \quad v_x=V_x, & \quad v_z=V_z, & \quad T=T_b \\
 z=z_1, & & & \quad T=T_{\text{entry}}
 \end{aligned} \tag{32}$$

For the solid polymer the characteristic items are the heat transport in the  $y$  and in the  $z$  directions, together with heat conduction in the  $y$  direction, hence:

$$\rho_s C_P \left( V_{sy} \frac{\partial T}{\partial y} + V_s \frac{\partial T}{\partial Z} \right) = k_s \frac{\partial^2 T}{\partial y^2} \tag{33}$$

with limiting values of:

$$\begin{aligned}
 z=0 & \quad T=T_0(y) \\
 y=0 & \quad T=T_0 & \quad V_{sy} = -V_{sy1} \\
 y=H_s & \quad T=T_0 & \quad V_{sy} = -V_{sy2}
 \end{aligned} \tag{34}$$

The velocity of the solid bed, assuming a rigid polymer is derived from the relationship:

$$V_s = \frac{Q}{\rho_s} H_0 W \tag{35}$$

by taking into account the actual density of the polymer.

The mass balance, characteristic to the melting process for the length  $\Delta Z$  is given by the following three equations:

$$Q_{|z+\Delta z} = Q_{|z} - Q_{y|z} + Q_{bx|z} + \omega_m \tag{36}$$

$$Q_{bz+\Delta z} = Q_{b|z} - Q_{bx|z} + Q_{sx|z} + \omega_b \tag{37}$$

$$Q_{s|z+\Delta z} = Q_{s|z} - Q_{sx|z} + Q_{y|z} + \omega_s. \tag{38}$$

For the solid bed the relationship is:

$$Q_{s|z+\Delta z} = Q_{s|z} - (\omega_m + \omega_b + \omega_s). \tag{39}$$

The heat flows for the boundary surfaces as follow:

— for the barrel surfaces:

$$k \frac{\partial T}{\partial y} \Big|_{b;\text{melt}} - k_s \frac{\partial T}{\partial y} \Big|_{h;\text{solid}} = \rho_s A V_{sy1} \tag{40}$$

— for the screw surfaces:

$$k_s \frac{\partial T}{\partial y} \Big|_{s;\text{solid}} - k \frac{\partial T}{\partial y} \Big|_{s;\text{melt}} = \rho_s A V_{sy2} \tag{41}$$

— while the melting rates give the reduction of the width of the solid bed

$$\omega = \rho_s W_s V_{sy} \Delta z \quad (42)$$

The energy balance,  
in the  $x$  direction:

$$\left( \frac{\partial P}{\partial x} \right)^b + \left( \frac{\partial P}{\partial x} \right)^s = \frac{2(\tau_{yx|} + \tau_{yx|b})}{H} \quad (43)$$

in the  $z$  direction:

$$\left( \frac{\partial P}{\partial z} \right)^b = \left( \frac{\partial P}{\partial z} \right)^s = \frac{\partial P}{\partial z} \quad (44)$$

The forces acting upon the surfaces of the solid polymer is given by:

$$\left( \frac{\partial P}{\partial x} \right)^b W_s = \left( \frac{\partial P}{\partial x} \right)^s (W_s + H_s) \quad (45)$$

The break-up criteria is given by:

$$\sigma_t \leq \frac{\Delta M}{K_n W_s H_s^2} = \frac{2m-1}{m} \frac{DK_b \cos \Phi \Delta z - (D-2H)K_s \cos \Theta \Delta z}{H_s^2} \quad (46)$$

where:  $K_b$  and  $K_s$  represent the shearing stresses in the  $z$  direction in the case of the melt layer, while  $K_s$  in the case of the cooled screw it designates the pressure and the friction constants at the screw surfaces.  $H_s$  represents the height of the solid bed, assumed to be homogeneous. In case the solid polymer is not regarded as homogeneous, or cannot be regarded as homogeneous, the right hand side of the equation (46) should constitute two members, the first member representing the melt layer thickness at the surfaces of the barrel and the thickness of the solid layer at the screw surfaces, respectively. These thicknesses may be determined from the temperature distribution developed in the solid polymer. The values of  $m$ , representing the properties of the material lies between the values of 1 to 1.3. The term  $\sigma_t$  is the break strength, in the case of compressed granules its value equals that of the pressure, this, in the case of the molten layer corresponds to the relationship  $a_1 E(1-T)T_m$ , relates to the modulus, where  $a_1 \approx 0.1$ .

It still need to be examined to find out whether a melt pool, filled with the melt is formed, or during the melting process merely the thickness of the solid bed is decreased. For this purpose it is necessary to include the forces acting on the solid polymer in a crosswise direction:

$$F_x \approx \left( \mu_b \frac{V_x}{\delta_b} - \frac{\delta_b}{2} \frac{\partial P_b}{\partial x} - \frac{\delta_s}{2} \cdot \frac{\partial P_s}{\partial x} - \frac{\partial P_b}{\partial x} H_s \right) W, \quad (47)$$

in case this forces are small a zone, filled by the melt, does not form. In such instances the functions related to the melt zone must be excluded from the system of equations, thus, the melting processes are characterized by a decrease of the solid bed height.

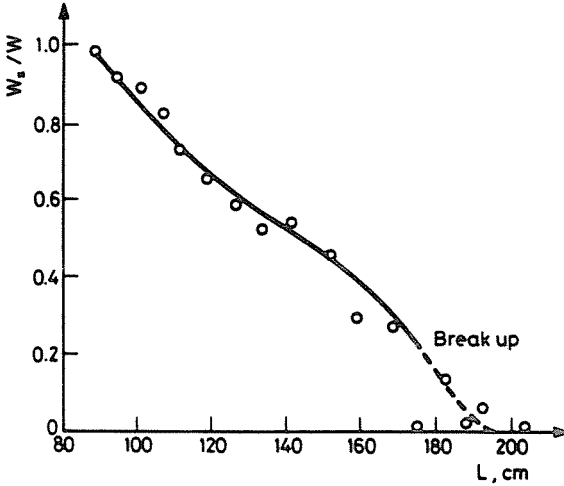


Fig. 3. Relative solid bed width profile for polyethylene,  
 $D = 60$  mm,  
 $Q = 17$  cm<sup>3</sup>/sec,  $T = 190^\circ\text{C}$ ,  $N = 40$  min<sup>-1</sup>.  
 ○ = experimental data,  
 — = calculated values

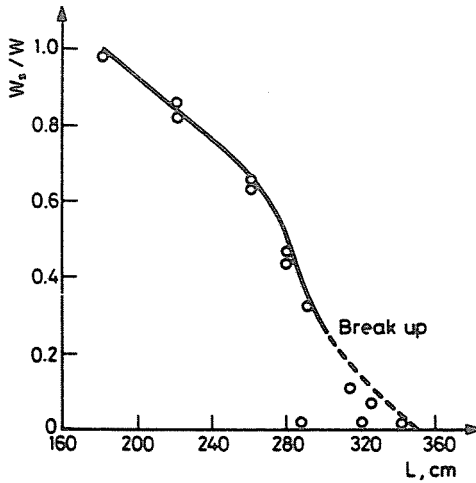


Fig. 4. Relative solid bed width profile for polypropylene,  
 $D = 60$  mm,  
 $Q = 2$  cm<sup>3</sup>/sec,  $T = 200^\circ\text{C}$ ,  $N = 10$  min<sup>-1</sup>,  
 ○ = experimental data,  
 — = calculated values

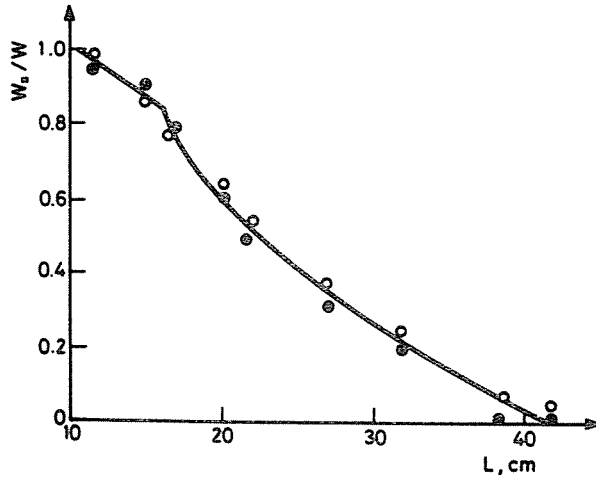


Fig. 5. Relative solid bed width profile for polymethylene,  
 $N = 4.2$  revs/min,  $Q = 7.83$  g/mm<sup>2</sup>,  
 $T_b = 155, 170$  and  $190^\circ\text{C}$ ,  
 — = calculated curve,  
 ○ and ● = experimental values

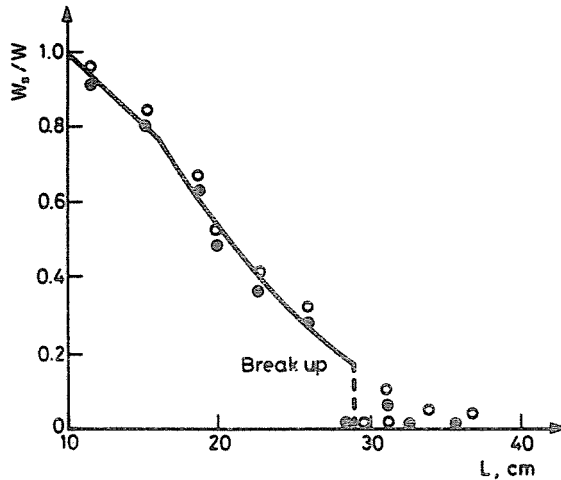


Fig. 6. Relative solid bed profile for polyethylene,  
 $N = 22.3$  revs/min  
 $Q = 26.5$  g/min,  $T_b = 155, 170$  and  $190^\circ\text{C}$ ,  
 — = calculated curve,  
 ○ and ● = experimental values

Solution of the system of equation is performed numerically step-by-step in an iterative cycle.

Figures 3 to 7 depict the width profiles of the solid material derived as a result of cooling experiments conducted versus calculated profile values

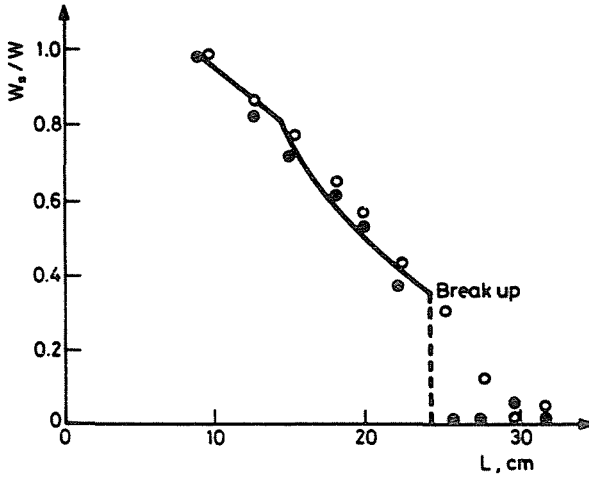


Fig. 7. Relative solid bed profile for polyethylene,  
 $N=46.4$  revs/min,  
 $Q=71.2$  g/min,  $T_b=155, 170$  and  $190^\circ\text{C}$ ,  
 — = calculated curve,  
 $\circ$  and  $\bullet$  = experimental values

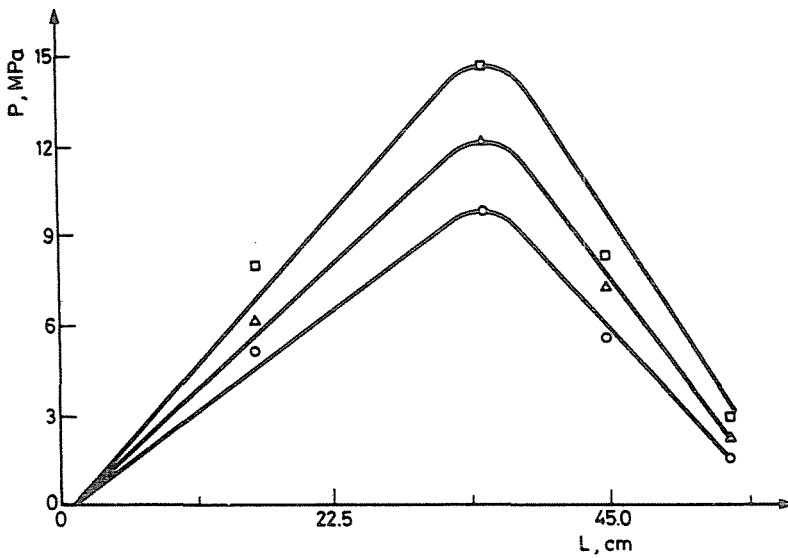


Fig. 8. Pressure profile.  
 $\circ$  2.2 revs/min,  
 $\triangle$  6.0 revs/min,  
 $\square$  15.0 revs/min

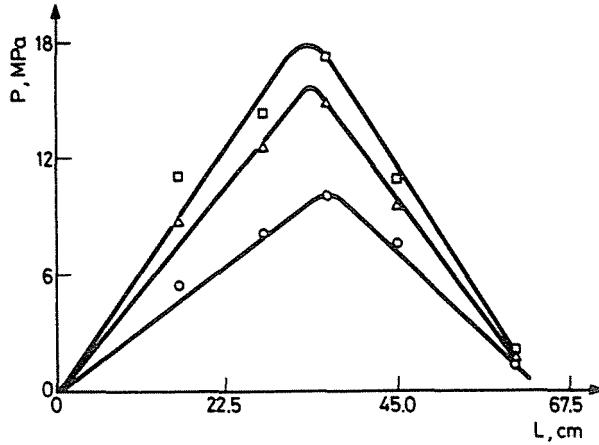


Fig. 9. Pressure profile.

- 1.2 revs/min,
- △ 3.7 revs/min,
- 10.5 revs/min

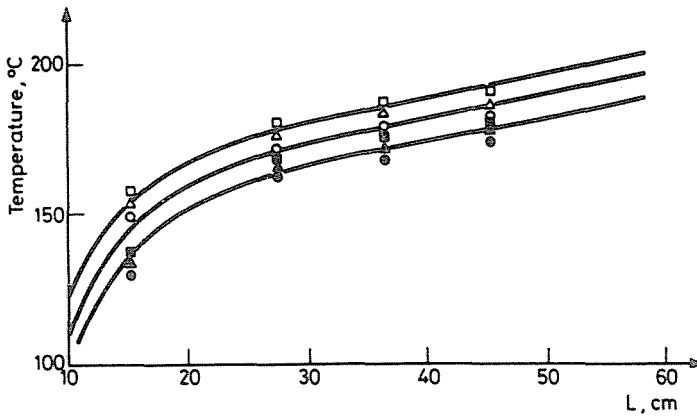


Fig. 10. Temperature profile:

Material: polyethylene

	Temperatures at the surfaces	Temperatures at the screw surfaces
1.2 revs/min	○	●
3.7 revs/min	△	▲
10.5 revs/min	□	■

derived. Figures 8 and 9 show the pressure profile determined experimentally, against calculated values. Figures 10 and 11 show the measured versus the calculated temperature profile arrived at.

The model described here estimates good the solid bed profile, pressure and temperature profile and gives the locate of break up.

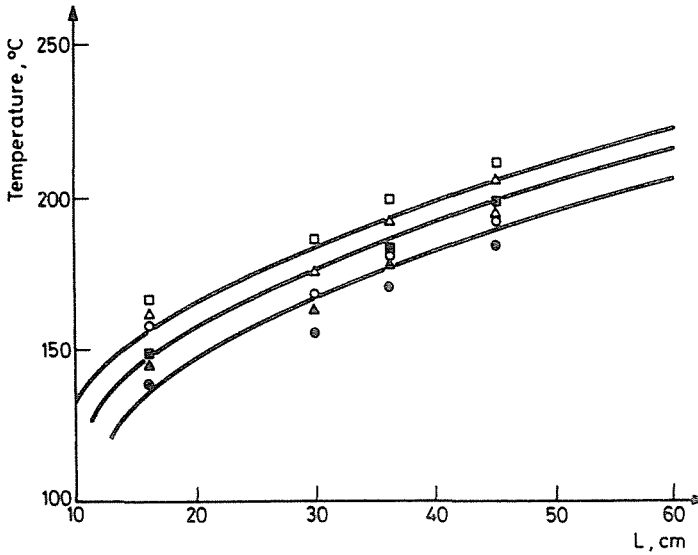


Fig. 11. Temperature profile:

Material: polyethylene

	Temperatures at the barrel surfaces	Temperatures at the screw surfaces
2.2 revs/min	○	●
6.0 revs/min	△	▲
15.0 revs/min	□	■

### References

1. MADDOCK, B. H.: SPE Journal 15, 983 (1959).
2. STREET, L. L.: Int. Plast. Engng. 1, 289 (1961).
3. TADMOR, Z.: Pol. Engng. Sci. 6, 185 (1966).
4. TADMOR, Z., DUVDEVANI, I. and KLEIN, I.: Pol. Engng. Sci. 7, 198 (1967).
5. MONDVAI, I., HALÁSZ, L. and MOLNÁR, I.: Plaste und Kautschuk 20, 630 (1973).
6. HALÁSZ, L.: Theory of extrusion of thermoplastics, computer simulation of the extruder processes. Doctorate theses, Budapest, 1976.
7. HALÁSZ, L.: Műanyag és Gumi 22 221 (1985).
8. EDMONSON, I. R. and FENNER, T.: Polymer 16, 19 (1975).
9. SHAPIRO, J., PEARSON, J. R. A. and HALMOS, A. L.: Polymer 17, 905 (1976).
10. SHAPIRO, J., HALMOS, A. and PEARSON, J. R. A.: Polymer 17, 912 (1976).
11. HALMOS, A. L., PEARSON, J. R. A. and TROTLOW, R.: Polymer 19, 1199 (1978).
12. KLENK, K. P.: Ph. D. theses, Aachen, 1969.
13. GALE, G. M.: Plastics and Polymers 38, 183 (1970).
14. CHUNG, D. I.: SPE Journal 32, 48 (1976).
15. LINDT, J. T.: Pol. Engng. Sci. 16, 284 (1976).
16. HINRICHS, D. R. and LILLELETH, L. U.: Pol. Engng. Sci. 10, 268 (1970).
17. VERMEULEN, J. R., SCARGO, P. G. and BEEK, W. G.: Chem. Engng. Sci. 26, 1457 (1971).
18. WERESSOVA, G. N. and KASANKOW, J. W.: Plaste und Kautschuk 24, 199 (1977).

19. DONOVAN, R. C.: *Pol. Engng. Sci.* 11, 247 (1971).
20. MOUNT, E. M., WATSON, J. G. and CHUNG, C. L.: *Pol. Engng. Sci.* 22, 729 (1982).
21. FUKASE, H. and KUNIO, T.: *Pol. Engng. Sci.* 22, 578 (1982).
22. PERWARDCHUK, V. P. and TRUFANOVA, N. M.: *Plaste und Kautchuk* 33, 102 (1986).
23. EBIRLI, B. and LINDT, J. T.: *Pol. Engng. Sci.* 24, 988 (1984).
24. LINDT, J. T. and EBIRLI, B.: *Pol. Engng. Sci.* 25, 412 (1985).
25. HALÁSZ, L.: *Rheological bases of the operational mode of screw plasticating units*, Ph. D. thesis, Budapest, 1987.
26. BASOV, N. I. and KAZANKOV, U. V.: *Injection moulding of polymers*, Himiya, Moscow, 1984.
27. KACIR, L., TADMOR, Z.: *Pol. Engng. Sci.* 12, 387 (1972).
28. HALÁSZ, L.: *Process controls and regulations applied in polymer processing*, Műszaki Könyvkiadó, Budapest, 1983.

L. HALÁSZ National Defence Research Institute, Budapest